Evaluating Visibility of Age Spot and Freckle based on Analysis and Synthesis of Facial Color Image

Misa Hirose[1)] , Yuri Tatsuzawa[2)], Saori Toyota[1)], Norimichi Tsumura[1)]
1) Graduate School of Advanced Integration Science, Chiba University, CHIBA, JAPAN
2) Department of Informatics and Imaging Systems, Chiba University, CHIBA, JAPAN

Abstract

In this research, we evaluate the visibility of age spot and freckle with changing the blood volume based on the actual facial color images and compare the result with that of pigmentation patterns generated by simulated spectral reflectance. We acquire the concentration distribution of melanin, hemoglobin and shading components by applying the independent component analysis on a facial color image. We reconstruct images by using the obtained melanin and shading concentration and the changed hemoglobin concentration to generate facial images with changing the blood volume. Finally, we evaluate the visibility of pigmentations using these images and compare with the result of pigmentation patterns based on simulated reflectance. In our previous study, we have already evaluated the visibility of pigmentation patterns, and the visibility became lower as the blood volume increases. However, we can see that a specific blood volume reduce the visibility of the actual pigmentations from the result of evaluating the skin color images.

Introduction

Skin is an organ that covers human body and affected by UV irradiation and aging. Age spot and freckle on human skin is caused by these affects. Since human face and skin receive a lot of attention in the human body, appearances of age and the health condition are caused by these pigmentations. Therefore, various studies to reduce the visibility of these pigmentations are performed in cosmetology and medical science.

Skin is a multi-layered tissue consists of epidermis, dermis and subcutaneous mainly. Skin color is determined by pigments such as melanin in the epidermis and hemoglobin in vessels of the dermis. Pigments such as β-carotene and bilirubin are also contained in the skin and make the skin color yellowish. It is known that age spot and freckle are the region that melanin in epidermis is excessively generated and the color of these pigmentation is darker than normal skin.

Lihong Wang and Steven L. Jaques produced a standard C-code for Monte Carlo simulation of light transport in multi-layered tissue (MCML) [1]. MCML is a technique for analyzing the color of the skin from the concentration of pigments by simulating photon propagation in multi-layered tissue. Tsumura *et al.* produced independent component analysis of skin color image [2]. We can obtain the concentration distribution of pigments such as melanin and hemoglobin from skin image by this method. Thus, we can mutually analyze skin color and the concentration of pigments based on these methods. We have already evaluated the relationship between the visibility and concentration of pigments by simulated spectral reflectance [3]. However, the relationship is not well understood on actual face. If we find that the reduction of the visibility of age spot and freckle on face is involved in the concentration of pigments, we can apply to develop cosmetics.

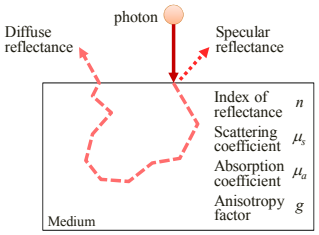

Figure 1. *The movement of photon through a medium calculated by Monte Carlo simulation.*

In this research, therefore, we evaluated the visibility of age spot with changing the blood volume by using facial color images and compare the result of facial color images with that of simulated spectral reflectance. The facial color image with changing blood volume is made by changing concentration of hemoglobin, where we acquired the concentration by applying independent component analysis on the image. We perform subjective evaluation for the visibility of the age spot and freckle patterns generated from simulated spectral reflectance and the facial color images. Finally, we evaluated the result and our simulated result. In this paper, the summary of [3] is described in the following section.

Monte Carlo Simulation for Photon Migration

Our research utilized Monte Carlo simulation of light transport in multi-layered tissue (MCML) to simulate the spectral reflectance of normal skin, age spot and freckle. MCML is constituted by following the propagation of photons in tissue.

As shown in Fig.1, a photon is launched into the tissue. The position of the photon is represented by the Cartesian coordinate (x, y, z) and initialized to $(0,0,0)$. The direction of photon movement is specified by the directional cosines (μ_x, μ_y, μ_z) and the initial value is $(0,0,1)$. Propagation distance of photons Δs is computed by $-In(\xi)/(\mu_a + \mu_s)$ where ξ is an uniform random number from 0 to 1, μ_a and μ_s are absorption and scattering coefficients respectively. The new photon position (x', y', z') are calculated as follows.

$$x' = x + \mu_x \Delta s,\ y' = y + \mu_y \Delta s,\ z' = z + \mu_z \Delta s \qquad (1)$$

The weight of each photon is assigned a weight, W, and initialized to 1. When the photon hit the tissue surface, the photon weight is decremented by the specular reflectance R_{sp}. When the photon propagated into a tissue with a different index of refraction, the probability that the photon will be internally reflected is defined by the Fresnel reflection coefficient. If the photon is propagated

into the tissue, the photon weight is reduced by the absorber. The attenuation of the photon weight is computed by absorption coefficient μ_a and scattering coefficient μ_s. After that, the photon is scattered. The scattering direction is determined by a normalized phase function describes the probability density function for a deflection and an azimuthal angle (θ,φ) . The probability distribution for the cosine of the deflection angle, $\cos\theta$, is characterized by Henyey-Greenstein phase function as follows.

$$\cos\theta = \frac{1}{2g}(1+g^2 - \frac{1-g^2}{1-g+2g\xi}), \tag{2}$$

where ξ is an uniformly distributed random number from 0 to 2π, the value of g is the anisotropy factor of scattering. The anisotropy factor characterizes the type of scattering. If an angle (θ,φ) at which photon is scattered are determined, the new direction (μ_x', μ_y', μ_z') are calculated by

$$\begin{aligned}
\mu_x' &= \frac{\sin\theta}{\sqrt{1-\mu_z^2}}(\mu_x\mu_z\cos\varphi - \mu_y\cos\varphi) + \mu_x\cos\varphi \\
\mu_y' &= \frac{\sin\theta}{\sqrt{1-\mu_z^2}}(\mu_y\mu_z\cos\varphi - \mu_x\cos\varphi) + \mu_y\cos\varphi \\
\mu_z' &= -\sin\theta\cos\varphi(1-\mu_z^2) + \mu_z\cos\varphi.
\end{aligned} \tag{3}$$

The diffuse reflectance is calculated by the ratio between the sum of weights that escape from the surface and initial weights.

Four-Layered Model for Human Skin

We generate four-layered skin model composed of stratum corneum, epidermis, papillary dermis and reticular dermis to simulate the spectral reflectance by MCML [4]. Figure 2 shows the skin model. We set the thickness t, index of refraction n, scattering coefficient μ_s, anisotropy factor g and absorption coefficient μ_a for each layer [5]. The scattering coefficient μ_s and anisotropy factor g are the same value for each layer and shown in Fig.3(a). Anisotropy factor g is approximated as follows.

$$g = 0.62\times(0.92\times10^{-3})\lambda. \tag{4}$$

The absorption coefficient μ_a is defined by the absorption coefficient and concentration of pigments. In this research, we consider six kinds of pigments, eumelanin and pheomelanin in the epidermis, oxyhemoglobin, deoxyhemoglobin and bilirubin in the papillary dermis and reticular dermis and β-carotene in all layer. The absorption coefficients of eumelanin $\mu_{a.eu}$ and pheomelanin $\mu_{a.pheo}$ are shown in Fig.3(b). These absorption coefficients are approximated as follows [6].

$$\begin{aligned}
\mu_{a.eu} &= 6.6\times10^{11}\times\lambda^{-3.33} \\
\mu_{a.pheo} &= 2.9\times10^{15}\times\lambda^{-4.75},
\end{aligned} \tag{5}$$

where λ is the wavelength of light in nanometers. The absorption coefficients of oxyhemoglobin, deoxyhemoglobin, β-carotene and bilirubin are calculated by using the molar extinction coefficients shown in Fig.3(c),(d) as follows [4][7].

$$\begin{aligned}
\mu_{a.ohb} &= 2.303\times S\times\frac{\varepsilon_{ohb}}{66500}c_{hb} \\
\mu_{a.car} &= 2.303\times\frac{\varepsilon_{car}}{66500}c_{car} \\
\mu_{a.bil} &= 2.303\times\frac{\varepsilon_{bil}}{66500}c_{bil},
\end{aligned} \tag{6}$$

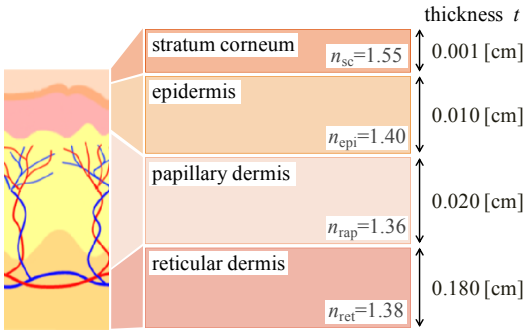

Figure 2. *Four-layered skin model.*

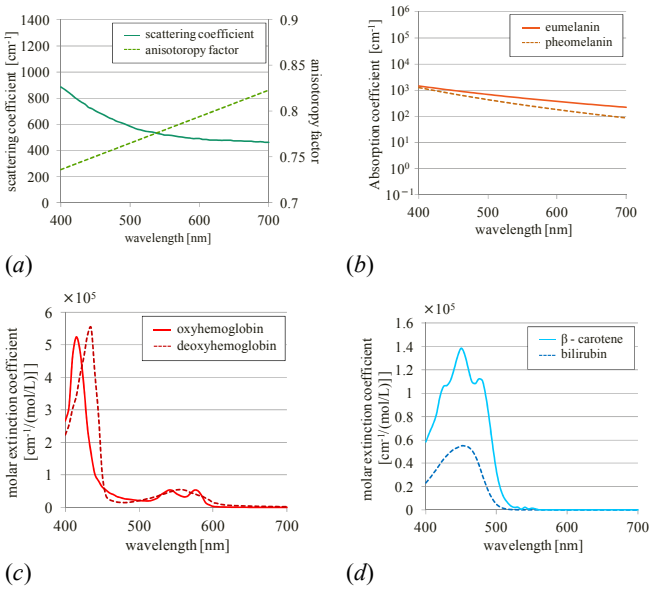

Figure 3. *(a) is scattering coefficient and anisotropy factor, (b) is absorption coefficient of eumelanin and pheomelanin, (c) is molar extinction coefficients of β-carotene and bilirubin, (d) is molar extinction coefficients for oxyhemoglobin and deoxyhemoglobin.*

where ε_{ohb}, ε_{car} and ε_{bil} are the molar extinction coefficients, $\mu_{a.ohb}$, $\mu_{a.car}$ and $\mu_{a.bil}$ are the absorption coefficients, c_{hb}, c_{car} and c_{bil} are the concentration, 66500, 537 and 585 are molecular weight, and S is oxygen saturation. The subscript *hb*, *ohb*, *car* and *bil* indicate hemoglobin, oxyhemoglobin, β-carotene and bilirubin. The absorption coefficient of deoxyhemoglobin ε_{dhb} is computed by replacing ε_{ohb}, S for ε_{dhb}, $(1-S)$ in Eq.6. The concentration of hemoglobin c_{hb} is typically 150[g/L].

The absorption coefficients for each layer $\mu_{a.sc}$, $\mu_{a.epi}$ and $\mu_{a.der}$ are computed as follows [4]. The subscript *sc*, *epi* and *der* indicate stratum corneum, epidermis and dermis respectively.

$$\begin{aligned}
\mu_{a.sc} &= \mu_{a.base} + \mu_{a.cs} \\
\mu_{a.epi} &= (M_{eu}\mu_{a.eu} + M_{pheo}\mu_{a.pheo})M + (\mu_{a.base} + \mu_{a.ce})(1-M) \\
\mu_{a.der} &= (\mu_{a.ohb} + \mu_{a.dhb} + \mu_{a.cd} + \mu_{a.bil})B + (\mu_{a.base} + \mu_{a.ce})(1-B),
\end{aligned} \tag{7}$$

where $\mu_{a.base}$ is the absorption coefficient of baseline skin such as organelles, cell membranes and fibrils, $\mu_{a.cs}$, $\mu_{a.ce}$ and $\mu_{a.cd}$ are the

© 2014 Society for Imaging Science and Technology

absorption coefficient of carotene in stratum corneum, epidermis and dermis respectively, M is the volume fraction of melanosomes in epidermis, M_{eu} and M_{pheo} are the volume fraction of eumelanin and pheomelanin in melanosomes, B is the volume fraction of whole blood in dermis. The absorption coefficient of baseline skin $\mu_{a.base}$ is approximated as follows [8].

$$\mu_{a.base} = 7.84 \times 10^{8} \times \lambda^{-3.255}. \quad (8)$$

Generating Age Spot and Freckle patterns from Simulated Spectral Reflectance [3]

The Concentration of Pigments for Skin, Age Spot and Freckle

We determined the concentration of pigments for normal skin, age spot and freckle to calculate spectral reflectance by MCML. The concentration of pigments for normal skin was determined such that simulated spectral reflectance approaches the average of measured spectral reflectance for 59 Japanese women. The oxygen saturation S was 75%, the concentration of β-carotene c_{car} and bilirubin c_{bil} were indicated in Table 1 [9]. Therefore, we determined the volume fraction of melanosomes M, eumelanin M_{eu}, pheomelanin M_{pheo} and whole blood B from the average spectral reflectance.

The measured spectral reflectance and the result of simulating by MCML are shown in Fig.4, where the volume fraction of melanosomes was epidermis M is 3.0%, the volume fraction of eumelanin M_{eu} and pheomelanin M_{pheo} in melanosomes were 10.0% and 90.0% respectively and the volume fraction of whole blood in dermis B was 3.0%. The color difference ΔE between measured and simulated spectral reflectance was 0.923 in CIELAB color space. It is known that we cannot perceive the difference between two colors if the value of ΔE is less than from 1 to 3 [10]. Thus, the result of simulation is close to the measured spectral reflectance.

We set the volume fraction of melanosomes M for age spot and freckle more than that for normal skin 3.0%, because age spot and freckle are the regions where melanin is excessively generated in epidermis. In this research, we set the volume fraction of melanosomes M for age spot and freckle to 4.0, 5.0 and 6.0%. For computing spectral reflectance with changing blood volume, we increased the blood volume for skin, age spot and freckle from 3.0% to 20.0%.

Generating Age Spot and Freckle patterns

We generated age spot and freckle patterns from spectral reflectance computed by MCML. First, we converted the spectral reflectance to XYZ color system as follows.

$$\begin{aligned} X &= k\int_{400}^{700} R(\lambda)P(\lambda)\bar{x}(\lambda)d\lambda \\ Y &= k\int_{400}^{700} R(\lambda)P(\lambda)\bar{y}(\lambda)d\lambda \\ Z &= k\int_{400}^{700} R(\lambda)P(\lambda)\bar{z}(\lambda)d\lambda \\ k &= 1/\int_{400}^{700} P(\lambda)\bar{y}(\lambda)d\lambda, \end{aligned} \quad (9)$$

where $R(\lambda)$ is spectral reflectance of skin, age spot and freckle, $P(\lambda)$ is spectral distribution of the light source and $x(\lambda)$, $y(\lambda)$, $z(\lambda)$ are color-matching function with a 2° view as the observation condition [11]. The spectral distribution of light source $P(\lambda)$ is 1.0 at all wavelength. Next, we convert these to RGB as follows.

$$\begin{pmatrix} R \\ G \\ B \end{pmatrix} = \begin{pmatrix} 2.3655 & -0.8971 & -0.4683 \\ -0.5151 & 1.4264 & 0.0887 \\ 0.0052 & -0.0144 & 1.0089 \end{pmatrix}. \quad (10)$$

We performed gamma correction with $\gamma = 2.4$ based on the gamma characteristics of display. As shown Fig.5, we generated 3 kinds of spatial distribution. The size of images is 500×500 (250,000 pixel), and age spot and freckle is 14,400 pixel. We applied a Gaussian filter to blur the boundary of skin and age spot. The Gaussian filter was defined by the kernel size and sigma σ. We set the kernel size 10×10 and $\sigma = 10$.

Table1 The concentration of β-carotene and bilirubin for each layer.

	β-carotene[g/L]	bilirubin[g/L]
stratum corneum	22.2×10^{-4}	
epidermis	22.2×10^{-4}	
papillary dermis	7.00×10^{-4}	7.00×10^{-3}
reticular dermis	7.75×10^{-4}	7.00×10^{-3}

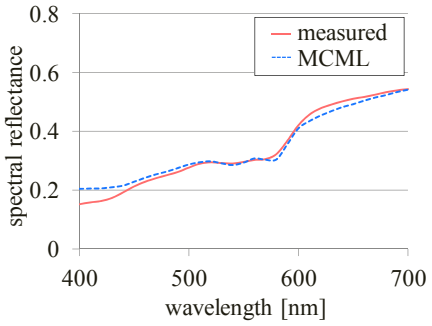

Figure 4. *Measured spectral reflectance and the result of simulation.*

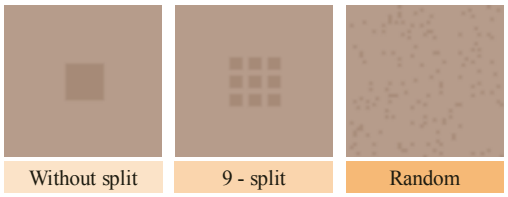

Figure 5. *The 3 kinds of distribution of age spot and freckle.*

Generating Skin Color Image with Changing Blood Volume based on Independent Component Analysis

Independent Component Analysis of Skin Color Image

We use the independent component analysis of skin color image proposed by Tsumura *et al*. to reproduce the color of real skin, age spot and freckle on the face with changing blood volume. As shown in Fig.6, we can acquire the concentration distribution of shading, melanin and hemoglobin using this technique [2]. We will describe this approach in this section.

Figure 7 is the skin model consists of epidermis and dermis. The skin color is denoted by melanin in the epidermis and hemoglobin in the dermis mainly. The light incident on the skin is separated into specular reflectance and diffuse reflectance. The specular reflectance indicates light source color, the diffuse reflectance indicates skin color. In this research, we consider the diffuse reflectance as observed signal and take the diffuse reflectance image of face based on a method proposed by Ojima *et al* [12]. The specular reflectance is removed by setting the polarizing filter orthogonally in front of camera and light source.

We show the relation of the skin model and the RGB value of the facial image. If we assume that Modified Lambert-Beer is satisfied, the diffuse reflectance of skin is shown as follows.

$$L(x,y,\lambda) = e^{-\rho_m(x,y)\sigma_m(\lambda)l_e(\lambda)-\rho_h(x,y)\sigma_h(\lambda)l_d(\lambda)}E(x,y,\lambda) \tag{11}$$

where $L(x, y, \lambda)$, $E(x, y, \lambda)$ are the spectral irradiance at (x, y) of the reflected and incident light, $\rho_m(x, y)$, $\rho_h(x, y)$ are the concentration of melanin and hemoglobin, $\sigma_m(x, y)$, $\sigma_h(x, y)$ are the absorption cross-section of melanin and hemoglobin, and $l_e(\lambda)$, $l_d(\lambda)$ are optical path length of light passing through the epidermis and dermis. Sensor response of a digital camera as the observed signal $v_i(x, y)$ is expressed as follows.

$$v_i(x,y) = k\int e^{-\rho_m(x,y)\sigma_m(\lambda)l_e(\lambda)-\rho_h(x,y)\sigma_h(\lambda)l_d(\lambda)}E(x,y,\lambda)s_i(\lambda)d\lambda \tag{12}$$

where k, $s_i(\lambda)$ are the gain and spectral sensitivity of the digital camera, and $i = (R, G, B)$. Since the spectral sensitivity of skin has a high correlation to that of the camera, the spectral sensitivity of the camera $s_i(\lambda)$ is approximated to $\delta_i(\lambda)$ in a narrow frequency band. If the irradiance does not depend on the direction, the monochromatic light $E(x, y, \lambda)$ is expressed by $p(x, y)\overline{E}(\lambda)$. Thus, Eq.12 is rewritten by Eq.13.

$$v_i(x,y) = ke^{-\rho_m(x,y)\sigma_m(\lambda)l_e(\lambda)-\rho_h(x,y)\sigma_h(\lambda)l_d(\lambda)}p(x,y)\overline{E}(\lambda_i) \tag{13}$$

We convert the RGB color space to the optical density space as follows.

$$\boldsymbol{v}^{log}(x,y) = -\rho_m(x,y)\boldsymbol{\sigma}_m(\lambda) - \rho_h(x,y)\boldsymbol{\sigma}_h(\lambda) + p^{\log}(x,y)\boldsymbol{1} + \boldsymbol{e}^{log}$$

where

$$\begin{aligned}
&\boldsymbol{v}^{log}(x,y) = [\log(v_R(x,y)), \log(v_G(x,y)), \log(v_B(x,y))]^T \\
&\boldsymbol{\sigma}_m = [\sigma_m(\lambda_R)l_e(\lambda_R), \sigma_m(\lambda_G)l_e(\lambda_G), \sigma_m(\lambda_B)l_e(\lambda_B)]^T \\
&\boldsymbol{\sigma}_h = [\sigma_h(\lambda_R)l_d(\lambda_R), \sigma_h(\lambda_G)l_d(\lambda_G), \sigma_h(\lambda_B)l_d(\lambda_B)]^T \\
&\boldsymbol{1} = [1,1,1]^T \\
&\boldsymbol{e}^{log} = [\log(E(\lambda_R)), \log(E(\lambda_G)), \log(E(\lambda_B))]^T \\
&p^{\log}(x,y) = \log(p(x,y)) + \log(k)
\end{aligned} \tag{14}$$

The observed signal $\boldsymbol{v}^{\log}$ is expressed by the bias vector $\boldsymbol{e}^{\log}$ and the weighted linear combination of $\boldsymbol{\sigma}_m$, $\boldsymbol{\sigma}_h$ and $\boldsymbol{1}$. The relation of observed signal and three independent signals is shown in Fig.8. The skin color is distributed on a two-dimensional plane consists of the vector of melanin and hemoglobin component. These vectors are obtained by performing an independent component analysis on the observed signal. We remove the shading information by projecting the skin color vector on the two-dimensional plane along the shading vector, and acquire the concentration of melanin and hemoglobin by projecting the two-dimensional plane on the vector of each pigment.

Figure 6. *The result of applying the independent component analysis on the skin color image*

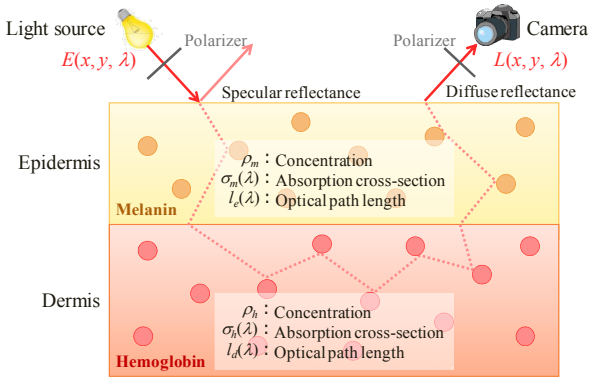

Figure 7. *The two-layered skin model and the movement of photon incident on the skin.*

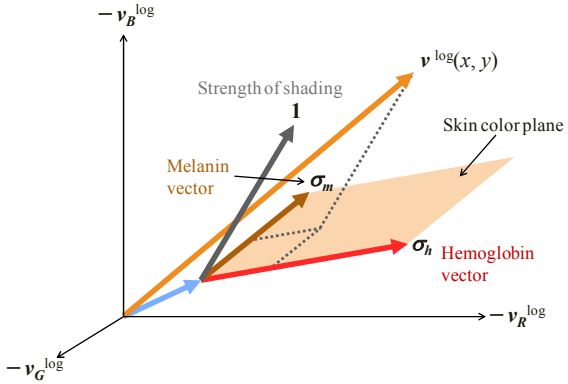

Figure 8. *The relationship of independent signal and three observation signal in the skin model*

Generating Skin Color Image with Changing Blood Volume

In this section, we show the process of generating skin color image with changing blood. First, we acquire the concentration distribution of shading, melanin and hemoglobin by the independent component analysis. We change the concentration of hemoglobin from −5% to +20%. We reconstruct the skin color image using these concentrations of pigments. At last, we perform gamma correction based on the gamma characteristics of display.

© 2014 Society for Imaging Science and Technology

Evaluating the Visibility of Pigmentations

Subjective Evaluation Method

Figure 9(a) shows the experimental room covered with black-out curtain. The display is 19 inch LCD and the viewing distance was approximately 87 cm that corresponded with three times the height of the display.

In the subjective evaluation, we utilized the method of paired comparison. Two images are displayed side-by-side at random on display, and the ratio of images and the display is shown in Fig.9(b). Observers select an image that age spot and freckle is less noticeable. We evaluated the result by Thurstone case V scaling. In the subjective evaluation of the pigmentation patterns and facial color images, the number of observers is 10 and 12 respectively.

Result and Discussion

Figure 10 shows 27 images of age spot and freckle pattern generated from spectral reflectance simulated by MCML. The melanin volume of age spot and freckle are 4.0, 5.0 and 6.0%, and the blood volume of skin, age spot and freckle are 3.0, 10.0 and 20.0%. There are 3 types of the spatial distribution of age spot and freckle, that is without split, 9-split, and random. Figure 11 shows the result of subjective evaluation for images shown in Fig.10. The vertical axis indicates the visibility of age spot and freckle. This value becomes larger as the visibility of the pigmentations decreases. The horizontal axis is the image numbers corresponding to those in Fig.10. The color of the bar chart indicates the blood volume of skin, age spot and freckle. From the results, we could see that the age spot and freckle become less noticeable, regardless of the spatial distribution and melanin volume of those, as the blood volume increases. We focused on the effect of increasing the blood volume on the reduction of visibility when the melanin volume is 4.0% and 6.0%. If the spatial distribution is without split, the effect is larger compared to random when the melanin volume is 4.0%. When the melanin volume is 6.0%, the effect is opposite to the above. If we want to reduce the visibility of age spot and freckle, therefore, the increase of the blood volume is effective in the case of without split when the amount of these pigments is low. In contrast, the increase of the blood volume is effective in the case of random when the color of these pigments is dark.

Figure 12 shows 6 images of facial image with the change of the blood volume and Fig.13 shows the result of subjective evaluation for images shown in Fig.12. The left vertical axis indicates the same evaluated value as Fig.11, and this value becomes larger as the visibility of the pigmentations decreases. The right vertical axis indicates the color difference of pigmentations and skin. The color difference is computed by using the average color of the region of skin and pigmentations. The horizontal axis is the image numbers corresponding to those in Fig.12. From Fig.13, we can see that the visibility of age spot and freckle is the lowest in the case of the amount of change in blood volume +5%. However, the color difference of pigmentations and skin is smaller as the blood volume increases. We think that perception of the color difference became difficult because the color of the actual skin is non-uniform unlike the images of age spot and freckle pattern generated by MCML.

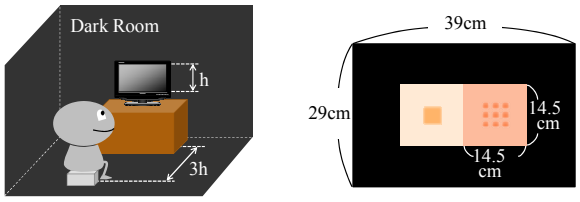

Figure 9. *(a) is experimental room. (b) is the ratio of display to images.*

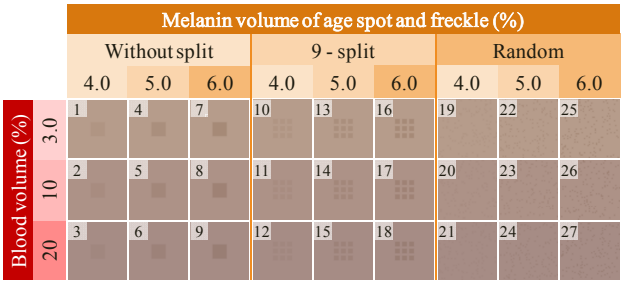

Figure 10. *Generated images of age spot and freckle pattern.*

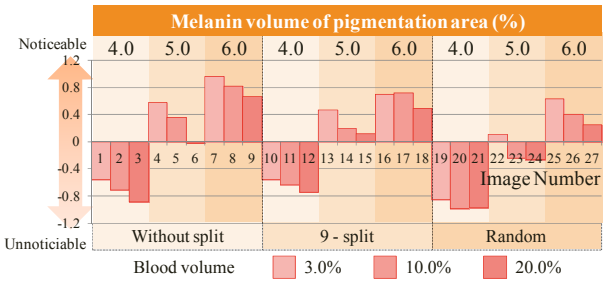

Figure 11. *The result of subjective evaluation for age spot and freckle patterns.*

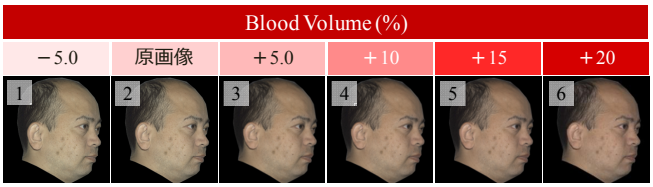

Figure 12. *Facial images with changing blood volume.*

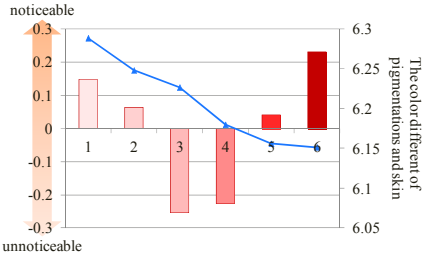

Figure 13. *The result of subjective evaluation for the facial images and the color difference of skin and pigmentations.*

Conclusion

In this research, we evaluate the visibility of age spot and freckle with changing blood volume based on the actual facial color images and compare the result with that of pigmentation patterns generated by simulated spectral reflectance. In our previous study, the result of evaluating the pigmentation patterns indicated that the visibility becomes lower as the blood volume increases. We could also see that the effect of increasing the blood volume on the reduction of visibility varies depending on the melanin volume and spatial distribution of these pigmentations. However, the result of evaluating the actual facial color images shows that a specific blood volume reduce the visibility of age spot and freckle. The color of the skin, age spot and freckle is actually non-uniform and different from the images generated by simulated spectral reflectance. Therefore, it is necessary to find a specific blood volume to reduce the visibility of the actual pigmentations. In the future work, we investigate the effect of the color unevenness of skin, age spot and freckle.

Acknowledgement

This research is partly supported by JSPS Grants-in-Aid for Scientific Research (24560040)

References

[1] Wang L. and Jacques S. L., "Monte Carlo Modeling of Light Transport in Multi-layered Tissues in Standard C", University of Texas M. D. Anderson Cancer Center (1992).

[2] Norimichi Tsumura, Nobutoshi Ojima, Kayoko Sato, *et al.*, "Image-based skin color and texture analysis/synthesis by extracting hemoglobin and melanin information if the skin", ACM Transactions on Graphics, Vol.22, No.3, 770-779 (2003).

[3] M. Hirose, S. Toyota, Y. Tatsuzawa and N. Tsumura, "Evaluating Visibility of Age Spot and Freckle based on Simulated Reflectance of Skin", Multispectral Colour Science (2014) (accepted).

[4] Aravind Krishnaswamy and Gladimir V.G. Baranoski, "A Biophysically-Based Spectral Model of Light Interaction with Human Skin", EUROGRAPHICS, Vol.23, No.3, pg.331-340 (2004)

[5] N. Tsumura, M. Kawabuchi, H. Haneishi and Y.Miyake, "Mapping pigmentation in human skin from multi-channel visible spectrum image by inverse optical scattering technique", Journal of Imaging Science and Technology, Vol.45, No.5, pg.444-450 (2000).

[6] Donner, C. and Jensen, H.W., "A Spectral BSSRDF for Shading Human Skin", EUROGRAPHICS, pg.409-417 (2006).

[7] Oregon Medical Laser Center, http://omlc.ogi.edu/.

[8] Jacques S. L., "Skin Optics", Organ Medical Center News, http://omlc.ogi.edu/news/jan98/skinoptics.html (1998).

[9] Anders Vahlquist, M.D. *et al*. "Vitamin A in Human Skin: II Concentrations of Carotene, Retinol and Dehydroretinol in Various Compornents of Normal Skin", Journal of Investigative Dermatology, Vol.79, No.2, pg.94-97 (1982).

[10] R. W. G. Hunt, "Measuring Color" (1998)

[11] Colour Matching Functions, http://cvrl.ioo.ucl.ac.uk/cmfs.htm.

[12] N. Ojima, T. Minami, and M. Kawai, "Transmittance measurement of cosmetic layer applied on skin by using processing", Proceeding of The 3rd Scientific Conference of the Asian Societies of Cosmetic Scientists, vol.114 (1997).

© 2014 Society for Imaging Science and Technology